13th IEA Heat Pump Conference
April 26-29, 2021 Jeju, Korea

Effect of shape change in the flow dirction of mini-channel on the flow patterns

Haruki Mitarai[a], Tetsuya Kobayashi[a], Koji Enoki[a], Kosaku Nishida[b] and Ikuro Akada[b*]

[a]The University of Electro-Communications 1-5-1, Chofugaoka, Chohu-shi, Tokyo 182-8585, Japan
[b]MAYEKAWA MFG. CO. LTD 2000, Tetsuzawa, Moriya-shi Ibaraki 302-0118, Japan

Abstract

As a method of improving the heat transfer of vapor-liquid two-phase flow in a mini-channel, there is the method of changing the shape. However, in previous researches, only the channel cross-sectional shape has been changed. In this study, the flow patterns of vapor-liquid two-phase flow in a plate heat exchanger with straight and wavy mini-channel was visualized, and the effect of changing the shape in the flow direction and the prospects for improving the heat transfer characteristics of the heat exchanger were investigated. A visualization experiment showed that imbalance in the liquid film thickness in the annular flow region of the wavy mini-channel in the flow direction. The thickness of the liquid film in the wavy mini-channel was measured and it was found that the thickness of the liquid film in the thin sections was less than half of that in the straight mini-channel and that in the thicker sections it was about 1.4 times thicker than that in the straight mini-channel. Then the heat transfer coefficient of wavy channel was almost 1.53 times better than the straight one.

Keywords:Mini-channel, Heat transfer, Vapor-liquid two phase flow, Boiling

1. INTRODUCTION

Currently, global warming is becoming a problem on a global scale. The production and consumption of CFC which causes global warming was restricted by the Montreal Protocol in 1987 and the emission factor was fixed in the Kyoto Protocol in 1997. In addition, alternative CFC was restricted by the Kigali Revision of the Montreal Protocol in 2016, too. Under the circumstances, it is considered that the refrigerant used in the refrigerator and air conditioner shifts to natural refrigerant such as ammonia. However, it is desirable to minimize the amount of refrigerant in them for safety because ammonia is toxic. In addition, we can achieve not only safety but also heat exchangers can be smaller by reducing the amount of refrigerant in heat exchangers. Therefore, enhancing the heat transfer performance in heat exchangers is need.

The heat transfer performance in heat exchangers can be improved by using microchannels with a diameter of about 1 mm. The reason of this phenomena are the evaporation heat transfer which occurs by heat conduction through the liquid film (liquid film evaporation heat transfer) in the slug flow area because the smaller the tube diameter, the thinner the liquid film present on the tube wall in addition to nucleate boiling heat transfer and forced convective heat transfer which are the mechanism of boiling heat transfer in the conventional channels and since the tube diameter is small in the micro tube, the liquid film present near the tube wall becomes thinner and the densification the heat transfer area with respect to the flow path area is increased.

K. Enoki (2013) [1] conducted experiments on boiling heat transfer coefficient and pressure drop measurement for each mini-channels, which has circular, rectangular and triangular cross sections. R 410A was used as the refrigerant, and the flow direction were vertical upward, vertical falling and horizontal. It

* Corresponding author.
E-mail address: enoki.koji@uec.ac.jp.

has been found that the boiling heat transfer coefficient was good for both circular, rectangular and triangular mini-channels. The high heat transfer coefficient was maintained up to high quality and decreased rapidly after occurred dryout. However, it was reported that the local heat transfer coefficient was different depending on the cross section.

In this study, the vapor-liquid two-phase flow in a heat exchanger was visualized by changing the mini-channel shape in the flow direction from a straight to a wavy, and the effects on the flow patterns and whether it can be expected to improve the heat transfer characteristics were confirmed. In addition, the boiling heat transfer coefficient of a single mini-channel was experimentally examined to show how much better the boiling heat transfer coefficient of a wavy mini-channel is compared with that of a straight one.

2. EXPERIMENTAL SET-UP AND PRODURES

The fluid used in this study is HFE-7000. For calculating the physical property value, we used NIST's REFPROP ver9.1 [2].

2.1. Visualization of flow patterns of a heat exchanger with wavy mini-channels

Figure 1 presents the schematic diagram of the experimental set-up for visualization of flow patterns. The fluid leaving the tank was sufficiently cooled by the double-pipe heat exchanger and pumped out at a constant flow rate by the syringe pump. The fluid was sufficiently cooled again by the double-pipe heat exchanger and flowed into the Coriolis flowmeter to measured mass flow rate. After that, the fluid was heated to a predetermined vapor quality by the preheater and flowed into the test section. The refrigerant leaving the test section was cooled by the condenser and returned to the tank.

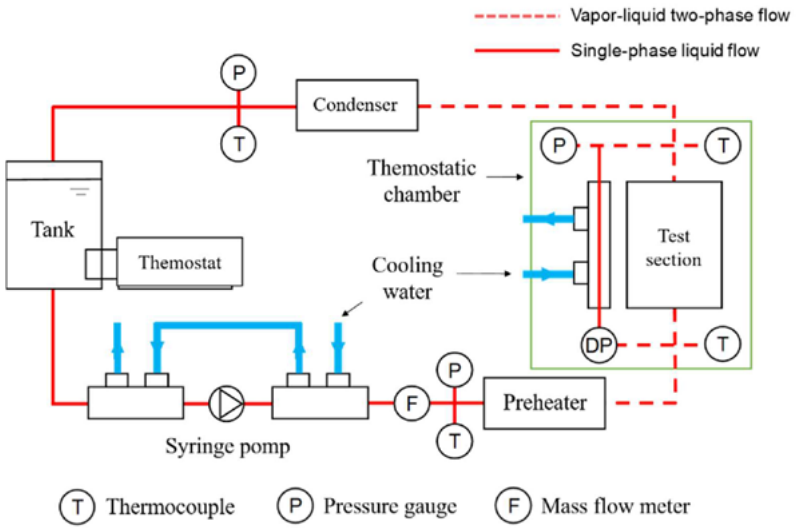


Fig. 1. Schematic diagram of experimental set-up for visualization

Two test sections were used in this study, one with a wavy and straight combined mini-channel and the other with only a straight mini-channel for comparison. The combined test section has wave-shaped in the upstream part and straight-shape in the downstream part channels, respectively. This combined test section is hereafter referred to simply as "wavy". Figure 2 shows a view of the wavy test section. The right figure of Fig. 2 shows the details of the test section when it is disassembled. As shown in these figures, the test section consisted of a glass for visualization, a metal plate made of stainless steel with a flow channel, a back plate with an inlet pipe, a back plate with an outlet pipe, and a copper plate, which were welded or bonded together. Flow channel plate is made of stainless steel in order to prevent corrosion even when ammonia is used as a refrigerant. The channels of the flow channel plate were created by etching. The visualization is achieved by mounting a glass in front of the flow channel plate and sealing it. The copper plate contains a cartridge

heater that directly heats the refrigerant flowing in the flow path uniformly by AC power. The refrigerant inlet is in the lower left corner and the outlet is in the upper center hole.

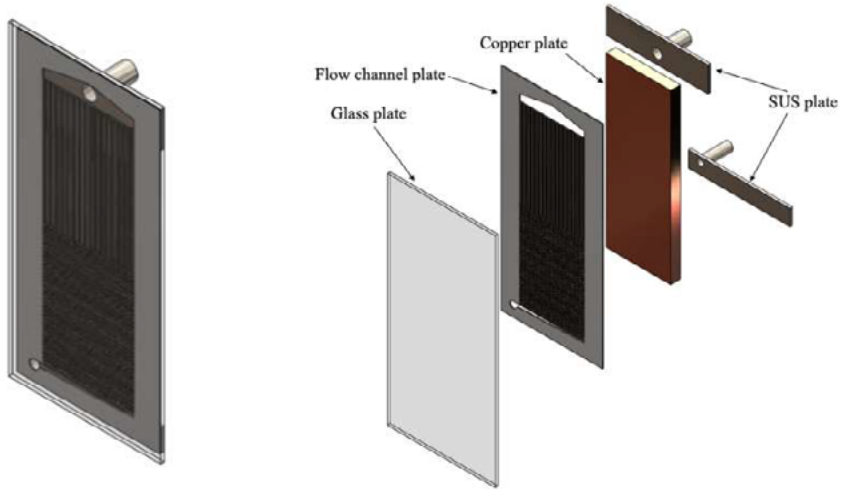


Fig. 2. Test section of wavy mini-channels

Figure 3 presents the schematic diagram of wavy mini-channels plate. Table 1 presents the specification of the wavy test section. The test unit processes 48 channels in a SUS304 plate. The flow path was structured such that the lower half was a wavy path with an amplitude of 0.4 mm and a wavelength of 4mm, and the upper half was a straight path. The right figure of Fig. 3 shows the details of the flow path of the test section. The width of the mini-channel was 1.49 mm and the width of the inlet of the mini-channel was 0.86 mm. The fluid flow was a vertical upward flow. The fluid flowed into the test section with an inlet quality of $x_{\text{in}} = 0.2$ and an outlet quality of $x_{\text{out}} = 0.9$. A high-speed camera was used to capture the flow of fluid in wavy paths. Red frames in Fig. 3 were the areas where videos were taken. The channel numbers are given from the inlet side and range from 1 to 48. The detailed locations of the red frames in Fig. 3 are, from left to right, channels 1 to 8 on the left side of the channel, 21 to 28 in the center of the channel, and 41 to 48 on the right side of the channel, and, from bottom to top, the inlet, 40 mm from the inlet, 132 mm from the inlet, and the outlet.

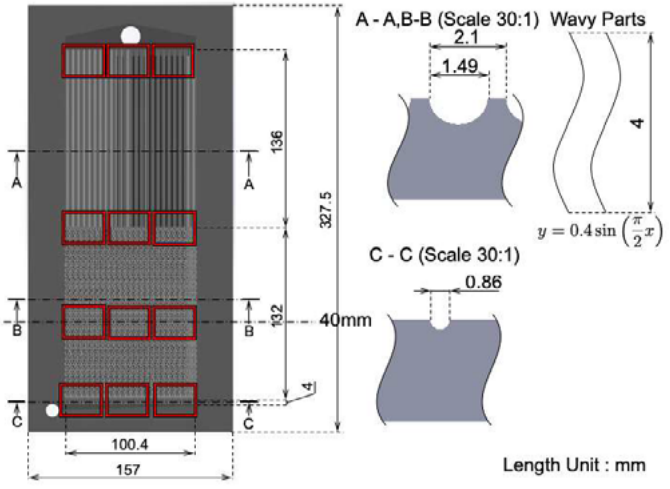


Fig. 3. Schematic diagram of wavy mini-channels plate

Table 1. Specification of wavy test section

	Flow path section	Choke section
Plate material	SUS316L	
Hydraulic diameter D[mm]	0.98	0.63
Flow area A[mm^2]	0.98	0.39
Wet perimeter l[mm]	4.02	2.46
Width d[mm]	1.49	0.86
Wavy amplitude a[mm]	0.4	
Wavelength of one wavy unit L[mm]	4	
The number of waves	33	1
Wavy line	$y = 0.4\sin(\frac{\pi x}{2})$	
The length of straight line [mm]	136	-
The length of wavy line [mm]	132	4
Number of flow paths	48	

2.2. Visualization of flow patterns of a heat exchanger with straight mini-channels

The visualization glass is installed in front of the flow channel plate, the heating method, the inlet and outlet ports, the direction of refrigerant flow, the shape of the inlet header, and shooting location are the same as for the wavy test section. The outlet header has a choke at the outlet end of the flow path to prevent backflow of the accumulated refrigerant. Figure 4 presents the schematic diagram of straight mini-channels plate. The right figure of Fig. 4 shows the details of the flow path of the test section. The width of the mini-channel was 1.59 mm and the width of the outlet of the mini-channel was 0.68 mm. Table 2 presents the specification of the straight test section

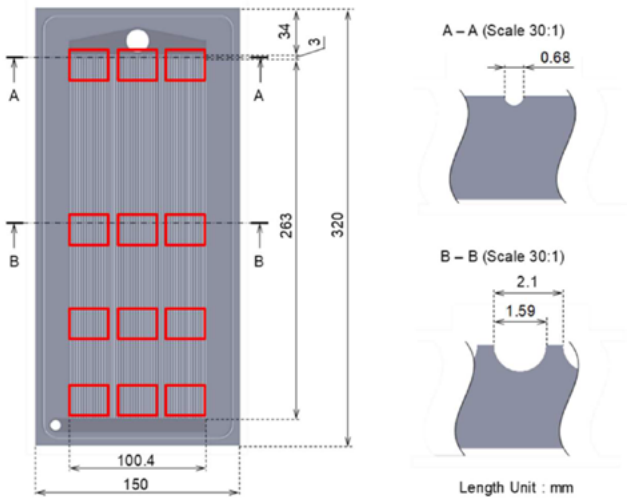


Fig. 4. Schematic diagram of straight mini-channels plate

Table 2. Specification of straight test section

	Flow path section	Choke section
Plate material	SUS316L	
Hydraulic diameter D[mm]	0.935	0.617
Flow area A[mm^2]	0.97	0.34
Wet perimeter l[mm]	4.14	2.22
Width d[mm]	1.61	0.69
Number of flow paths	48	

Table 3 presents the experimental conditions for the straight test section and the wavy test section.

Table 3. Experimental condition of test section

Refrigerant	HFE-7000
Saturation temperature [°C]	30
Absolute saturation pressure [MPa]	0.087
Mass flow rate M[kg/s]	0.002
Mass flux G [kg/(m^2 · s)]	40
Heat flux q [kW/m^2]	7.5
Latent heat Δh_v [kJ/kg]	135.5
Test section inlet quality x_{in}	0.2
Test section outlet quality x_{out}	0.9

The specific enthalpy of fluid mixing at the inlet and outlet of the test section was calculated based on the specific enthalpy at the inlet of the preheater, $h_{\text{PH in}}$. $h_{\text{PH in}}$ was determined from the pressure and temperature of the refrigerant in liquid single phase state measured at the inlet of the preheater. The specific enthalpy at the inlet of the test section, $h_{\text{TS in}}$, was calculated from the mass flow rate M, the electrical input at the preheater, Q_{PH}, and the heat gain from the inlet of the preheater to the inlet of the test section, Q_1, as shown in Equation (1). Furthermore, the specific enthalpy at the outlet of the test section, $h_{\text{TS out}}$, was calculated from the mass flow rate, M, the electrical input at the test section, Q_{TS}, and the heat gain from the inlet to the outlet of the test section, Q_2, as shown in Equation (2).

$$h_{\text{TS in}} = h_{\text{PH in}} + \frac{(Q_1 + Q_{\text{PH}}) \times 10^{-3}}{M} \tag{1}$$

$$h_{\text{TS out}} = h_{\text{TS in}} + \frac{(Q_2 + Q_{\text{TS}}) \times 10^{-3}}{M} \tag{2}$$

Using the values of Equations (1) and (2), the vapor quality x_{in} at the inlet of the test chamber and the vapor quality x_{out} at the outlet of the test chamber were calculated as shown in Equations (3) and (4) below. $h_{x=0}$ is the specific enthalpy of saturated liquid and Δh_v is the latent heat of evaporation of the refrigerant.

$$x_{\text{in}} = \frac{h_{\text{TSin}} - h_{x=0}}{\Delta h_v} \tag{3}$$

$$x_{\text{out}} = \frac{h_{\text{TSout}} - h_{x=0}}{\Delta h_v} \tag{4}$$

The quality errors at the inlet and outlet were calculated using the following equations (5) and (6).

$$\Delta x_{\text{in}} = \frac{(\Delta Q_1 + \Delta Q_{\text{PH}}) \times 10^{-3}}{M \times \Delta h_v} \tag{5}$$

$$\Delta x_{\text{out}} = \frac{(\Delta Q_2 + \Delta Q_{\text{TS}}) \times 10^{-3}}{M \times \Delta h_v} \tag{6}$$

The estimation errors for heat gain are $\Delta Q_1 = 0.00016\text{W}$ and $\Delta Q_2 = 0.00027\text{W}$, respectively. On the other hand, when we find the estimation error of each heater, we find that $\Delta Q_{\text{PH}} = 0.66\text{W}$ and $\Delta Q_{\text{TS}} = 1.5\text{W}$, which is large enough for the estimation error of heat gain. Therefore, the estimation error of each heater is dominant to the estimation error of quality. From the above, the quality errors at the inlet and outlet are calculated to be $\Delta x_{\text{in}} = 0.002$ and $\Delta x_{\text{out}} = 0.005$, respectively.

2.3. Measurements of boiling heat transfer coefficient

Figure 5 presents the schematic diagram of the experimental set-up for experimental investigation of boiling heat transfer coefficient in mini-channels. The fluid was pumped into the flow meter 1 and the flow rate was measured. Then, it branched in two directions, one goes to the test section and the other passes through the flow meter 2 and returned to the pump again. It was possible to adjust the flow rate of the fluid flowing to the test section accurately by adjusting the degree of opening of the valve before the preheater. The flow rate of fluid flowing to the test section was obtained by subtracting the value indicated by flow meter 2 from the value

indicated by flow meter 1. After that, the fluid heading for the test section was heated by the preheater. Afterward, the heat transfer coefficient was measured.

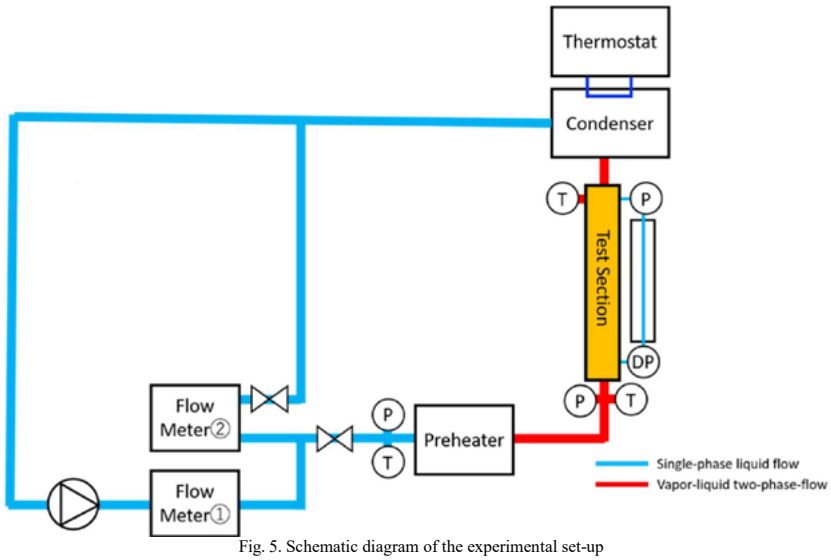


Fig. 5. Schematic diagram of the experimental set-up

Table 4 presents the specification of the mini-channels. The fluid was heated to a predetermined quality by the preheater and flowing into the test section. The temperature was measured at the test section inlet and outlet.

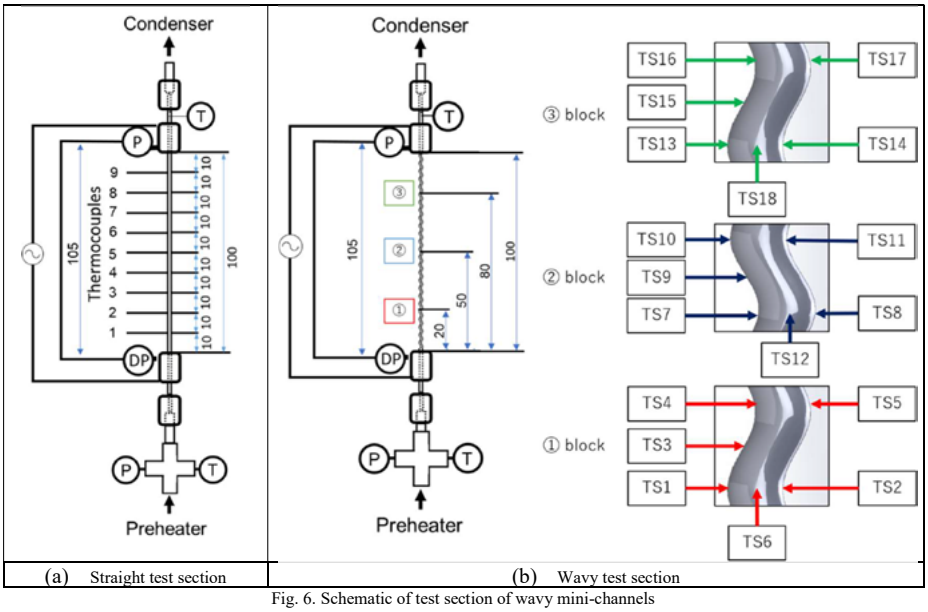
Table 4. Specification of the mini-channels

	Straight	Wavy
Material	SUS304	
Hydraulic diameter D[mm]	1.07	0.93
Flow area A[mm^2]	0.90	0.68
Differential pressure length [mm]	105	
Tube thick ness [mm]	0.29	
Thermal conductivity [W/(m · K)]	16.7	
Wave length L[mm]	-	4.0
Amplitude a[mm]	-	0.4

Figure 6 presents a schematic view of the test section of straight mini-channels and wavy mini-channels. The fluid was heated to a predetermined quality by the preheater and flowed into the test section. The test section was directly heated by AC power. Thermocouples were attached as shown in Fig. 6 in three areas of 20 mm, 50mm and 80 mm from below the wavy mini-channels and at nine locations 10 mm apart from the entrance to the exit of the straight mini-channels. Also, the test section was covered with a cylindrical heat insulating material and glass wool was packed inside to reduce the heat loss to the surroundings as much as possible. In the test section, experiments were conducted with constant heat flux, and the inlet quality of the test section was changed. Table5 presents the experimental conditions. Local heat transfer coefficient was calculated from

$$\alpha = \frac{q}{T_\mathrm{i} - T_\mathrm{b}} \tag{7}$$

T_i was the temperature of the inner wall of the mini-channel. Since the mini-channel was heated from an AC power, T_i was calculated from the heat conduction equation by using measured temperature of the outer wall, the thickness of the mini-channel used, heat flux and the thermal conductivity of SUS304 taking into account internal heat generation. T_b was the average temperature of fluid. It was calculated from the specific enthalpy and local pressure of the fluid at the location where the thermocouple was attached by using REFPROP.



(a) Straight test section (b) Wavy test section

Fig. 6. Schematic of test section of wavy mini-channels

Table 5. Experimental conditions of heat transfer measurement

Mass flux G [kg/(m^2 · s)]	40
Heat flux q [kW/m^2]	8
Quality x[−]	0 – 1
Saturation temperature[℃]	30

3. RESULTS AND DISCUSSION

3.1. Visualization of flow patterns in wavy mini-channels

Figure 7 shows the results of imaging of flow patterns at each location shown in Fig. 3 with a high-speed camera. In the inlet of the test section, slug flow was observed at channels of No.21 to No.28 and No.41 to No.48 and annular flow was observed at No.1 to No.8. In the area 40mm above the inlet of the test section, annular flow was observed at channels of No.1 to No.8 and No.41 to No.48 and slug flow was observed at No.21 to No.28. In other areas, annular flow was observed. It can be seen that the wavy area is filled with slug flow and annular flow. The annular flow has a high heat transfer rate in the tube forced convection boiling heat transfer. In the slug flow, liquid film evaporation heat transfer is generated by heat transfer through a thin liquid film in the mini-channels in addition to nucleate boiling heat transfer and forced convective heat transfer which are the mechanism of boiling heat transfer in the conventional channels. From this fact, it is considered the heat transfer performance of the wavy mini-channels is enhanced. Furthermore, flow disturbances were observed everywhere. Therefore, it is considered that the stretching and folding of the fluid elements by turbulence promotes fluid mixing and enhance heat transfer.

3.2. Visualization of flow patterns in straight mini-channels

Figure 8 shows the results of imaging the flow pattern of the straight test section at each of the locations shown in Fig. 4 with a high-speed camera. Annular flows were observed at the whole area of channels No.1 to No.8, slug flows in the inlet of the test section at channels No.21 to No.28 and No.41 to No.48, and annular flows in other areas. Back-flow was observed in channels No.45 to No.48, but it was only temporary.

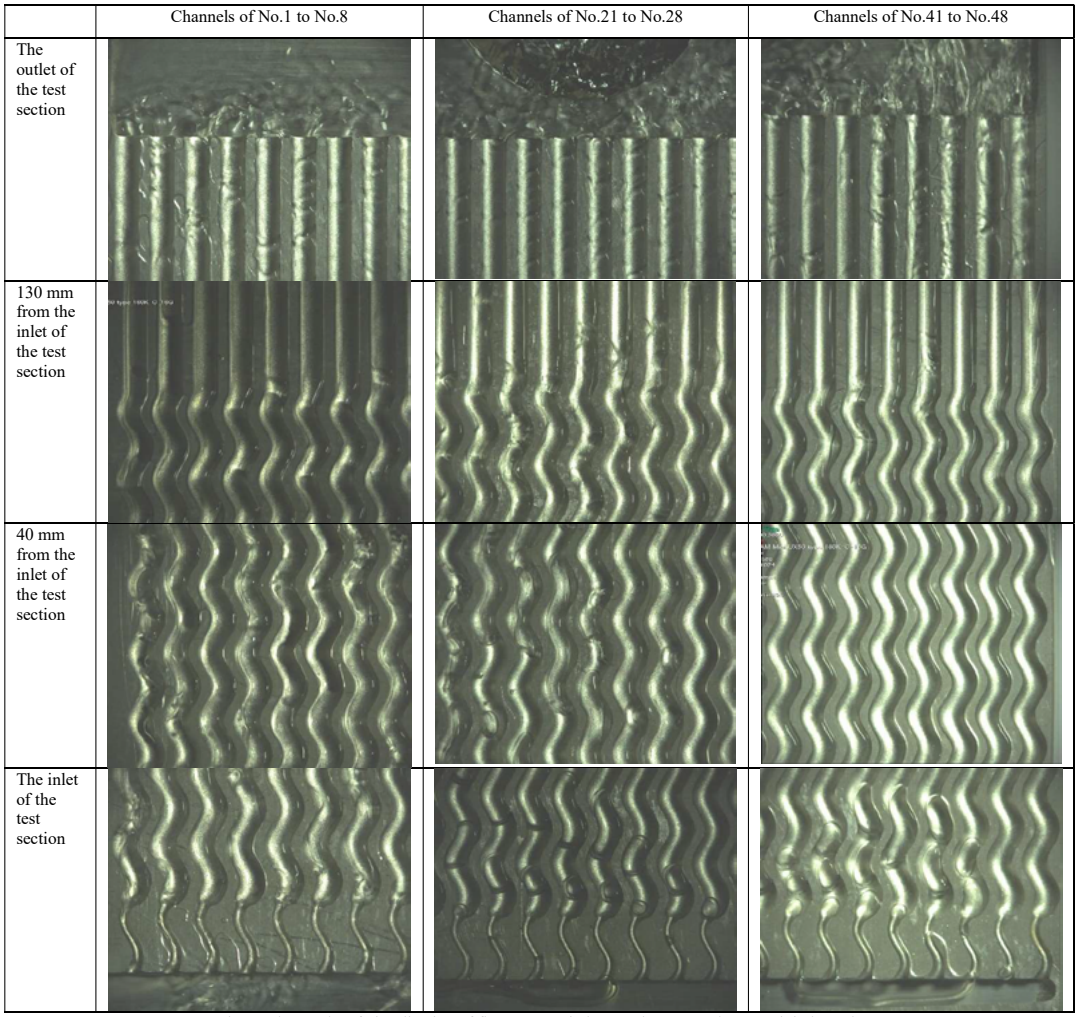


Fig. 7. The results of visualization of flow patterns in heat exchanger used wavy mini-channels

3.3. Effects of mini-channels shape change on the flow pattern and heat transfer coefficient

Enlarged images of the vapor-liquid two-phase flow in the straight test section and the wavy test section taken with a macro lens are shown in Figs. 9 and 10, respectively. The video images were taken at 132 mm from the channel entrance of channels No.21 to No.28 in the center of the test section. Figure 11 is the enlarged view of the red frame in Fig. 10. Figures 9 and 11 show that there is a clear bias in the thickness of the liquid film flowing through the channel wall in the annular channel region in the wavy channel compared to the straight channel, and that the liquid film is divided into thicker and thinner sections in the trough of the wavy mini-channel. In addition, it was found that the fluid is easily held in the trough of the wavy mini-channel and the liquid film is thick. Moreover, it turned out that thickness of liquid film is changing periodically as it became thicker and thinner in the points where it is thick. This phenomenon is considered to be due to the following mechanism. First, the liquid film grows and becomes thicker. After that, it breaks the surface tension of the channel wall and peels off as a droplet. Finally, the liquid film repeats the growth again. It can be seen that peeled droplets are believed to promote fluid mixing. On the other hand, the liquid film was very thin in other areas. Although liquid film evaporation heat transfer is originally observed in the

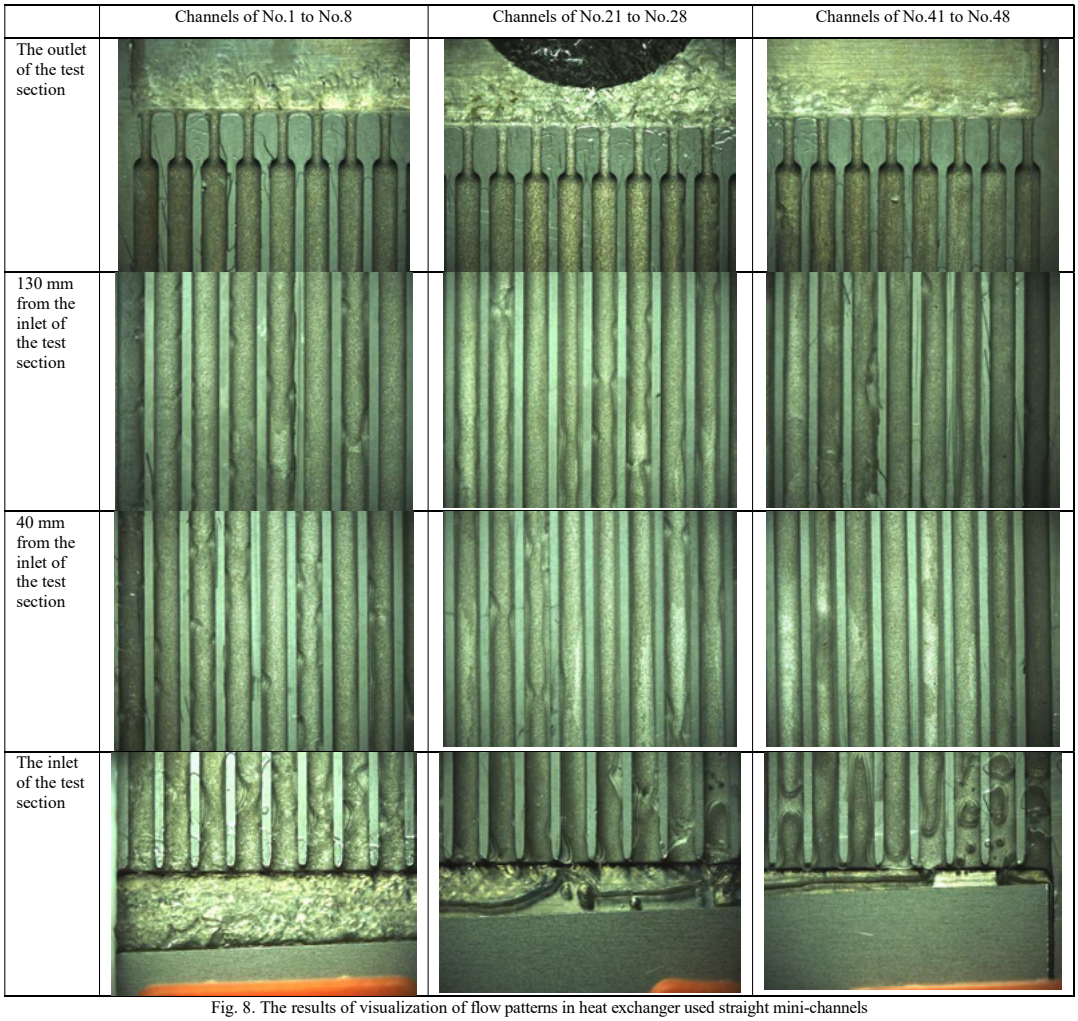


Fig. 8. The results of visualization of flow patterns in heat exchanger used straight mini-channels

slug flow area, since a very thin portion of the liquid film appears due to the thickness deviation of the liquid film, liquid film evaporation heat transfer is performed even in the annular flow area in wavy mini-channels. As a result, heat transfer performance is considered to be enhanced.

In order to estimate the thickness of the liquid film, measurements of the wall thickness of each channel were made using the video images. However, the thickness of the liquid film on the channel walls changed periodically in both straight and wavy channels. we measured the period of variation of the liquid film thickness at thicker points in the wave-shaped channel, and averaged the results of the measurement of the liquid film thickness within the period to obtain the average liquid film thickness as a parameter. In order to measure the period of the film thickness variation, images were taken at 132 mm from the channel entrance of the channel No.21 to No.28 (Fig. 8), where the film thickness variation was most clearly captured, by using a Photron FASTCAM Viewer 3. Table 6 shows the results of the measurement of the thickness variation period of the liquid film. The channel numbers are numbered 1 to 7, from left to right, for channels No.21 to No.28 in the center of the channel, as seen in the video taken at 132 mm from the channel entrance.

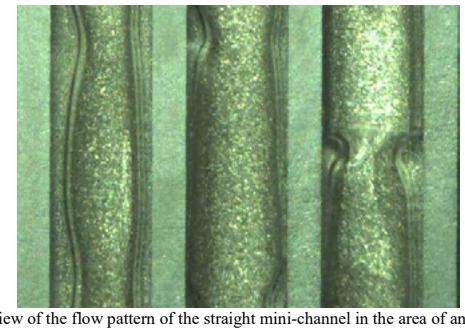


Fig. 9. View of the flow pattern of the straight mini-channel in the area of annular flow

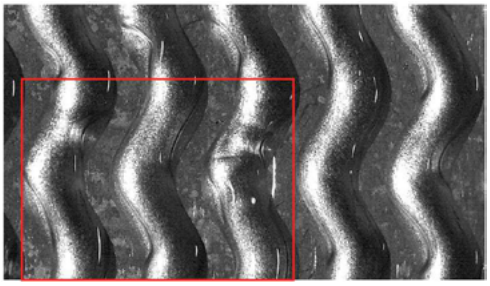


Fig. 10. View of the flow pattern of the wavy mini-channel in the area of annular flow

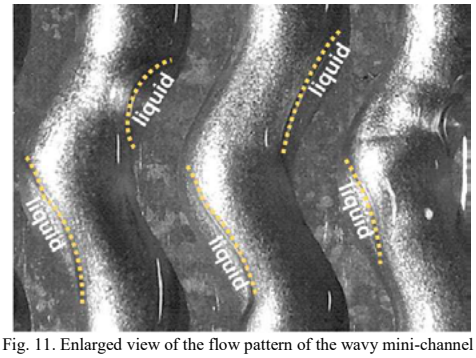


Fig. 11. Enlarged view of the flow pattern of the wavy mini-channel

Table 6. Fluctuation period of thickness of liquid film

Number of flow path	1	2	3	4	5	6	7
Fluctuation period of thickness of liquid film (frame, 1frame = 0.0005 s)	75.5 (0.038 s)	45.4 (0.023 s)	80.2 (0.040 s)	43.5 (0.022 s)	55.4 (0.028 s)	69.1 (0.035 s)	59.2 (0.030 s)

The average period of variation in the thickness of the liquid film was calculated by averaging the values in Table 6 to obtain 61.2. Therefore, the shooting speed used 60 frames out of 2000 fps as the approximate period of liquid film thickness variation, and measurements of 60 frames of liquid film thickness were made for both straight and wavy channels. Here, the period of liquid film thickness variation is 0.03 seconds. The wavy channel was divided into two sections, one where the film thickness was thicker and one where it was thinner, and the other where the film thickness was too thin to be measured, and the thickness of the wavy channel was measured for 60 frames. The area of the thickest liquid film in each frame was measured. The liquid film thicknesses were measured for 60 frames in the straight channel, the wavy channel where the film is thin, and the wavy channel where the film is thick, and averaged. The average liquid film thicknesses of the straight and wavy mini-channels are shown in Table 7. Table 7 shows that the liquid film thickness in

the wavy channel is about 1.4 times thicker than that in the straight mini-channel and less than half in the thin section.

Table 7. Average of thickness of liquid film

Straight	Wavy(thick parts)	Wavy(thin parts)
0.278mm	0.388mm	0.129mm

3.4. Boiling heat transfer coefficient in wavy mini-channels

Figure 12 shows that heat transfer coefficients at each position where thermocouples were attached. In addition, it is shown with heat transfer coefficients in straight mini-channels for comparison. As you can see from Fig. 12, the heat transfer coefficient at the mounting position of each thermocouple increases with increasing quality and it becomes maximum around the quality 0.45 and then drops. Therefore, it is considered that the dryout occurs at around the quality 0.45. In Fig. 12, the heat transfer coefficient is higher in the crest of the wavy mini-channels compared to the trough. From visualization experiments, it can be observed that the liquid film is thinner in the crest of the wavy mini-channels. These results suggest that the liquid film is thinner in the crest of the wavy mini-channels, which leads to liquid film evaporation heat transfer and thus improved heat transfer performance. The average heat transfer coefficients of the straight and wavy mini-channels before dryout are calculated as $\alpha = 1.73\mathrm{kW/(m^2 \cdot K)}$ for straight one and $\alpha = 2.65\mathrm{kW/(m^2 \cdot K)}$ for wavy one. Therefore, it can be seen that heat transfer coefficient of the wavy mini-chnnels was about 1.53 times better than that of straight one with the same cross section area of flow path.

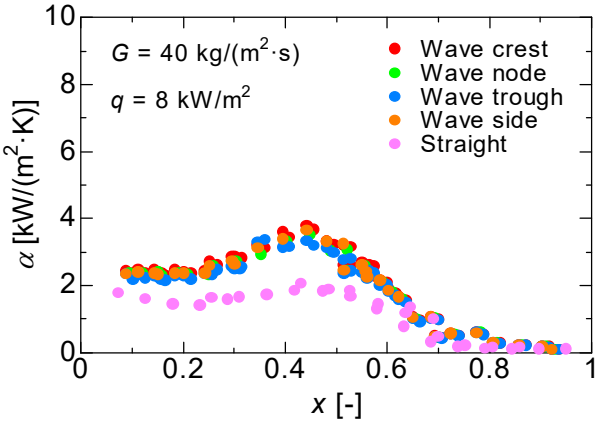


Fig. 12. Heat transfer coefficient at each thermocouple mounting position of the wavy mini-channel in $G = 40\ \mathrm{kg/(m^2 \cdot s)}$

4. CONCLUSIONS

In this study, the visualization of the flow pattern of vapor-liquid two phase flow in the wavy mini-channels and straight mini-channels were performed. In addition, in order to consider these, boiling heat transfer coefficient of wavy mini-channels and straight mini-channels were investigated experimentally. From the results of the experiment, we got the knowledge shown below.

(1) Compared to straight channels, there is a clear bias in the thickness of the liquid film flowing on the wall of the annular flow region in wavy channels. In addition, thickness of liquid film is changing periodically in the points where it is thick. As a result, heat transfer performance is enhanced by liquid film evaporation heat transfer not only in the slug flow region but also in the annular flow region. Furthermore, the disturbances observed may promote fluid mixing and contribute to improved heat transfer. The bias of the liquid film thickness in the wavy mini-channels is less than half of that in the straight mini-channels and about 1.4 times thicker in the thicker areas.

(2) Heat transfer coefficients in wavy mini-channels increase with increasing quality and it drop after becoming maximum. The heat transfer coefficient is improved in the crest where the liquid film in the wavy mini-channels is considered to be thin. In addition, heat transfer coefficients in wavy mini-channels before dryout show about 1.53 times better than that of straight mini-channels.

NOMENCLATURE

A	flow area	$[\mathrm{mm}^2]$
a	wavy amplitude	[mm]
D	hydraulic diameter	[mm]
d	Width	[mm]
G	mass flux	$[\mathrm{kg}/(\mathrm{m}^2 \cdot \mathrm{s})]$
Δh_v	latent heat	[kJ/kg]
$h_{x=0}$	the specific enthalpy of saturated liquid	[kJ/kg]
$h_{\mathrm{PH\ in}}$	the specific enthalpy at the inlet of the preheater	[kJ/kg]
$h_{\mathrm{TS\ in}}$	the specific enthalpy at the inlet of the test section	[kJ/kg]
$h_{\mathrm{TS\ out}}$	the specific enthalpy at the outlet of the test section	[kJ/kg]
M	mass flow rate	[kg/s]
L	wavelength of one wavy unit	[mm]
l	wet perimeter	[mm]
q	average heat flux	$[\mathrm{kW/m}^2]$
Q_1	the heat gain from the inlet of the preheater to the inlet of the test section	[W]
Q_2	the heat gain from the inlet to the outlet of the test section	[W]
ΔQ_1	The estimation errors for heat gain from the inlet of the preheater to the inlet of the test section	[W]
ΔQ_2	The estimation errors for heat gain from the inlet to the outlet of the test section	[W]
Q_{PH}	the electrical input at the preheater	[W]
Q_{TS}	the electrical input at the test section	[W]
ΔQ_{PH}	the estimation error of preheater	[W]
ΔQ_{TS}	the estimation error of test section	[W]
T_{i}	temperature of inner wall of the pipe	[℃]
T_{b}	average temperature of fluid	[℃]
x	quality	[−]
x_{in}	Test section inlet quality	[−]
x_{out}	Test section outlet quality	[−]
Δx_{in}	the quality errors at the inlet	[−]
Δx_{out}	the quality errors at the outlet	[−]

GREEK SYMBOLS

α	heat transfer coefficient	$[\mathrm{kW}/(\mathrm{m}^2 \cdot \mathrm{K})]$

References

[1] Koji ENOKI (2013): “Boiling Heat Transfer, Flow Patterns and Pressure Drop of the two-phase flow in small tubes”, Doctoral thesis UT51-2013-E770(In Japanese)

[2] Lemmon, E.W., Huber, M.L., McLinden, M.O. (2013): “NIST Reference Fluid Thermodynamic and Transport Properties – REFPROP Version 9.1”, NIST Standard Reference Database 23